Fabric induced weakness of tectonic faults

André Niemeijer,[1,2,3,4] Chris Marone,[2,3] and Derek Elsworth[1,3]

[1]   Mature fault zones appear to be weaker than predicted by both theory and experiment. One explanation involves the presence of weak minerals, such as talc. However, talc is only a minor constituent of most fault zones and thus the question arises: what proportion of a weak mineral is needed to satisfy weak fault models? Existing studies of fault gouges indicate that >30% of the weak phase is necessary to weaken faults - a proportion not supported by observations. Here we demonstrate that weakening of fault gouges can be accomplished by as little as 4 wt% talc, provided the talc forms a critically-aligned, through-going layer. Observations of foliated fault rocks in mature, large-offset faults suggest they are produced as a consequence of ongoing fault displacement and thus our observations may provide a common explanation for weakness of mature faults. **Citation:** Niemeijer, A., C. Marone, and D. Elsworth (2010), Fabric induced weakness of tectonic faults, *Geophys. Res. Lett.*, *37*, L03304, doi:10.1029/2009GL041689.

1.   Introduction

[2]   The apparent weakness of mature faults with large offsets (>5 km) and the state of stress in the Earth's crust have long been a matter of debate. The lack of a heat flow anomaly [*Lachenbruch and Sass*, 1980, 1992] and the orientation of principal stresses around major fault zones [*Zoback et al.*, 1987; *Zoback*, 2000] have been used to suggest that some tectonic faults slip under much lower resolved shear stress than inferred from "classical" rock mechanics experiments [*Engelder et al.*, 1975; *Dieterich*, 1978; *Marone et al.*, 1990]. Moreover, the existence of low angle normal faults (i.e., faults that dip at an angle <30 °) can only be explained by extreme fault zone weakness [*Collettini and Sibson*, 2001]. Possible explanations for weak faults include low effective stress, via elevated fluid pressures [*Rice*, 1992; *Faulkner and Rutter*, 2001], the presence of weak phyllosilicates or clays [*Imber et al.*, 2001; *Collettini and Holdsworth*, 2004; *Moore and Rymer*, 2007; *Collettini et al.*, 2009a], dynamic weakening [*Melosh*, 1996; *Di Toro et al.*, 2006; *Ampuero and Ben-Zion*, 2008], the operation of stress-enhanced dissolution-precipitation creep [e.g., *Rutter and Mainprice*, 1979] or a combination of these

[*Bos and Spiers*, 2002; *Niemeijer and Spiers*, 2005, 2006, 2007]. However, the origin of fault weakness remains poorly understood and a matter of much interest [*Scholz*, 2000].

[3]   Recent field observations of talc in both the San Andreas fault [*Moore and Rymer*, 2007] and an exhumed low angle normal fault in Italy [*Collettini et al.*, 2009b] have led to speculations that the weakness of these faults can be explained by the presence of talc, which has very low friction. However, considering that the San Andreas fault is over a 1000 km long and that only minor amounts (2–3 wt%) of talc were discovered, the question arises: how much talc is needed to satisfy weak fault models? Recent experiments on synthetic mixtures of talc and a second, strong phase (quartz sand) suggests that 30 to 50 wt% talc is needed [*Carpenter et al.*, 2009]. However, because of the layered structure of talc (high aspect ratio), this mineral is likely to form a through-going connected layer, which would significantly weaken the composite gouge as long as shear can be localized on the talc-bearing foliation. Indeed, recent experiments on foliated fault rocks [*Collettini et al.*, 2009a] show that fabric can induce significant weakness even under cataclastic conditions. Moreover, experiments on analogue fault gouges, using synthetic mixtures of salt and muscovite/kaolinite [*Bos and Spiers*, 2002; *Niemeijer and Spiers*, 2005, 2006] show that weakening can occur with as little as 10 wt% of the weak mineral, provided that the "strong" mineral deforms by pressure-solution and the weak mineral forms a through-going foliation. These experiments show that frictional slip can occur under low shear stress, provided that a weak and continuous foliation is present, which extends the slip importance of phyllosilicate-bearing foliated rocks into the brittle regime. Previous work under ductile deformation conditions has established the role of fabric in weakening due to the plasticity and inter-connectivity of ductile phyllosilicate phases [*Shea and Kronenberg*, 1993; *Wintsch et al.*, 1995]. However, the details of foliation development and the amount of material required to induce weakening under brittle, cataclastic conditions remain unclear.

[4]   We investigated the affect of fabric on fault strength in laboratory experiments conducted under tectonic stresses. Layers of synthetic fault gouge were composed of quartz and talc, and the role of fabric was examined by comparing layers containing thin zones of pure talc with layers formed from homogeneous mixtures of the two components. We report on the effects of talc interlayer thickness, normal stress, sliding velocity, and net strain on the strength of the composite gouges.

2.   Experimental Methods

[5]   Our friction experiments were conducted under room temperature and humidity (~20%) with the double-direct

[1]Department of Energy and Mineral Engineering, Pennsylvania State University, University Park, Pennsylvania, USA.
[2]Department of Geosciences, Pennsylvania State University, University Park, Pennsylvania, USA.
[3]G3 Center and Energy Institute, Pennsylvania State University, University Park, Pennsylvania, USA.
[4]Now at Istituto Nazionale di Geofisica e Vulcanologia, Rome, Italy.
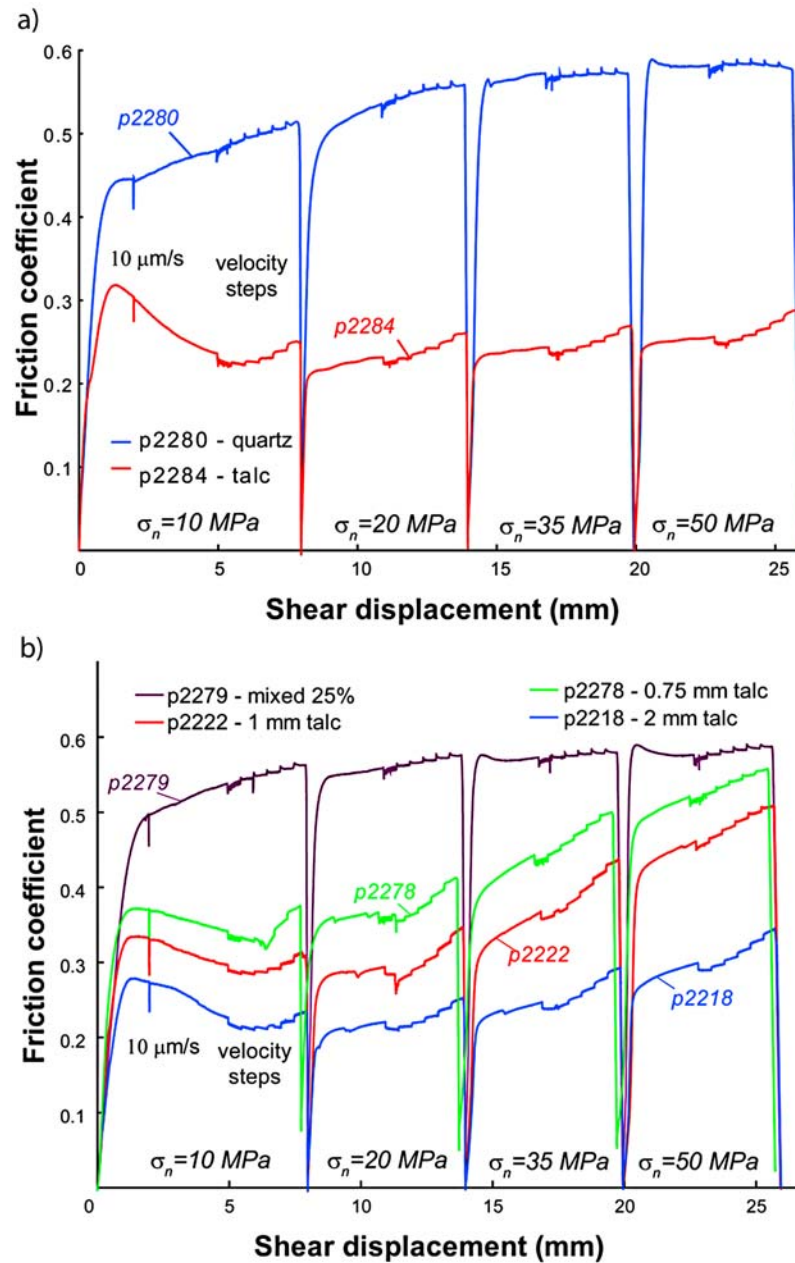
Figure 1. (a) Evolution of friction with shear displacement for the end-member cases (100% talc, p2284 and 100% quartz, p2280). Normal stress as indicated; velocity-stepping sequence is 1-3-10-30-100-300 μm/s for a displacement of 0.5 mm at each velocity. (b) Evolution of friction with shear displacement for four talc-quartz mixtures: three with a talc interlayer (0.75, 1 and 2 mm-thick) and one (p2279) in which 25 wt% of talc was mixed homogeneously with granular quartz. Normal stress and velocity history same as Figure 1a.

shear configuration at constant normal stress inside a servo-controlled, biaxial loading frame (for details, see auxiliary material) [*Scott et al.*, 1994; *Mair and Marone*, 1999; *Niemeijer et al.*, 2008].[1] We used Ottawa quartz sand (F110, U.S. Silica Company, average grain size of 127 μm) and, in a subset of experiments, blue sand (Kelly's Crafts, Ross, Ohio, U.S.A., average grain size 200 μm) which has similar frictional properties and provides contrast between the sand and talc to facilitate visual observations. The talc was from the Balmat mine, New York, USA provided by Ward's Natural Science and was crushed using a shatter box and sieved to <125 μm. After each experiment, the sample assembly was carefully taken apart in order to recover the sample. The talc layers were typically recovered intact, but the surrounding sand was not cohesive and could not be recovered.

3. Results

[6] Figure 1a shows the evolution of friction with shear displacement for the two end-member gouges in this study
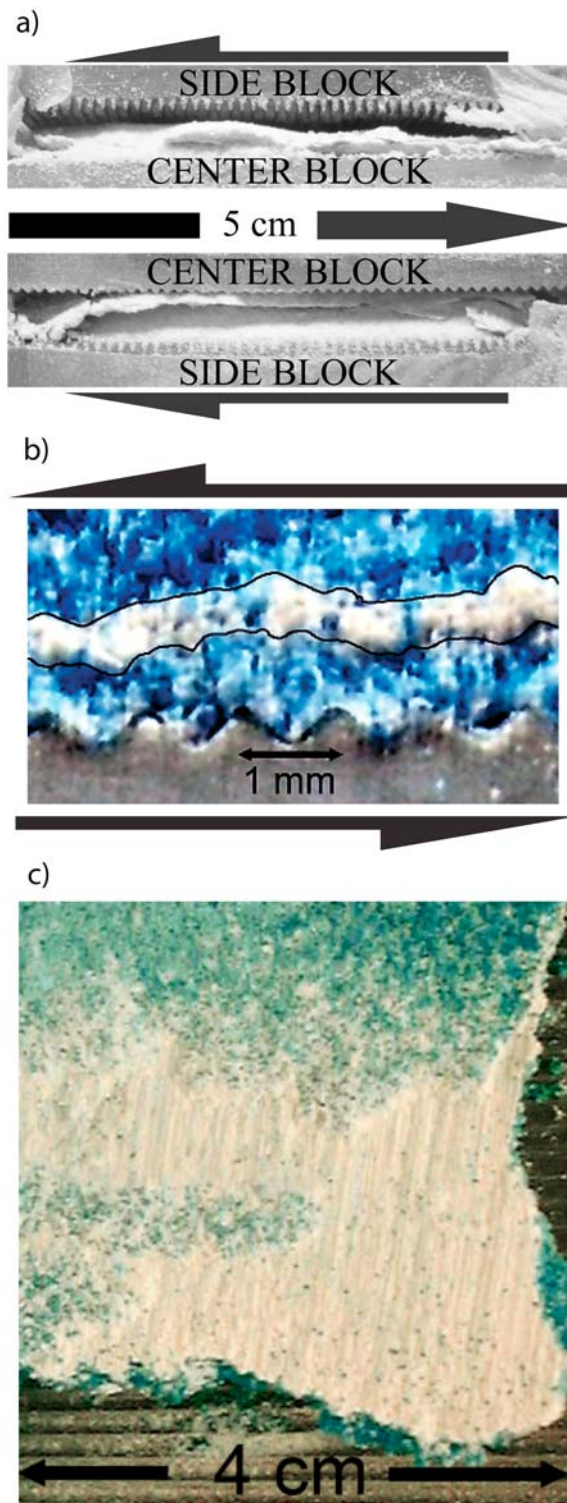
Figure 2. (a) Side-view of the sample assembly after shearing (experiment p2218, see Table 1 of Text S1 of the auxiliary material). Quartz was incohesive whereas the thin talc layer was cohesive (protuding layers) and strong enough to be preserved intact. (b) Zoomed side-view of the talc interlayer in an experiment with blue sand (p2221). Note undulations and evidence of flow pertubation folding within the talc interlayer. (c) Top view of talc interlayer surface (p2221). Striations are parallel to the shear direction (from top to bottom).

(i.e., 100% talc and 100% quartz), where the friction coefficient is defined as the measured shear stress divided by the measured normal stress. The pure talc sample (experiment p2284) shows an initial peak stress followed by a gradual weakening. In contrast, the quartz layer (p2280) shows a minor initial peak stress and continues to strengthen during shearing. Strain hardening is likely due to grain size reduction by cataclasis resulting in gouge densification and strengthening [*Marone et al.*, 1990]. The frictional strength for pure quartz (0.6) and pure talc (0.25) are consistent with results from other studies [*Marone et al.*, 1990; *Mair and Marone*, 1999; *Moore and Lockner*, 2008].

[7] The behavior of homogeneous mineral mixtures differs from layers that included a thin zone of talc (Figure 1b). Note that the relative amount of talc in the homogeneous mixture is larger than for experiments with talc interlayers (25 wt% *vs.* <16 wt% talc, see also Table 1 of Text S1 of the auxiliary material). The evolution of friction with shear displacement is a strong function of layer fabric. Homogeneous mixtures (p2279) exhibited a gradual roll-over in stress, without a peak stress value, followed by strain hardening until a steady state frictional strength was reached. Note that frictional strength of the mixture is very similar to that of pure quartz (Figure 1). In contrast, all samples with a talc interlayer were weaker than the homogeneous mixtures (Figure 1). Layers with a talc interlayer exhibited a peak in shear stress during initial loading, at the lowest normal stress, followed by gradual strain weakening (Figure 1). At higher normal stresses, these layers exhibited continuous strain hardening. We varied the location of the talc interlayer, from the centre to the edges of the composite layer, and found that it had a negligible effect (see auxiliary material).

[8] We investigated the effects of sliding velocity, normal stress, shear strain, grain size, and fabric orientation. For samples with talc interlayers, friction varied systematically with sliding velocity, in the range 1 to 1000 μm/s. Friction increased with increasing sliding velocity and the evolution of friction varied with velocity (see auxiliary material). Fabric orientation also had an important effect on frictional strength of composite layers. When the talc fabric was rotated toward the R1 Riedel shear orientation (~3° relative to the shearing direction), the strength of the composite layer was consistently lower (up to ~0.05 in friction) than when the talc zone was parallel to the shear direction (see auxiliary material).

[9] Post experiment inspection of the samples showed that the quartz was incohesive, whereas the talc interlayers were sufficiently cohesive to be recovered intact (Figure 2). Samples with a talc interlayer showed a tendency to develop a larger-scale fabric including a wavy, anastasmosing appearance of the talc interlayer ("flow perturbation folds"). The wavelength and amplitude was roughly 0.5–1 mm and 200 μm, respectively (Figure 2b). Talc interlayers also showed evidence of strong internal shear as evidenced by Riedel shear partings and as shear along the talc/gouge interface. The surfaces of the talc layer are characterized by a series of striations (similar to slickensides) oriented in the direction of shear (Figure 2c). The width and spacing of the striations is ~0.1 mm and 0.5 mm, respectively, which is consistent with smearing (scoring) by quartz grains from the surrounding material. The striations are more pronounced in experiments
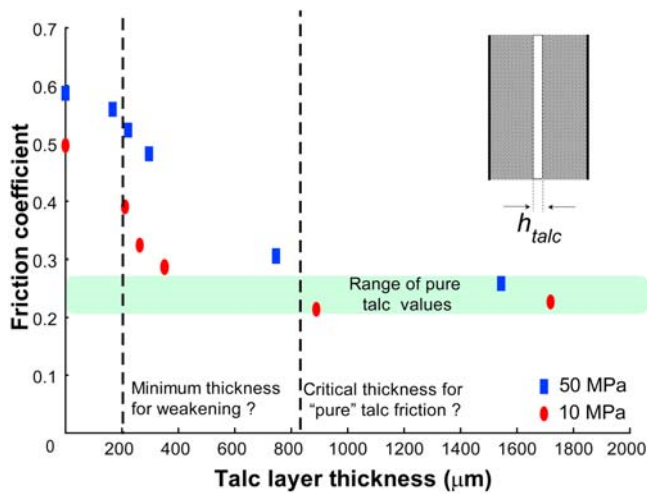
Figure 3. Plot of steady state friction (at v = 10 μm/s) vs. talc interlayer thickness. The value of talc interlayer thickness at each steady state was calculated assuming that the interlayer of talc thins and compacts as measured for pure talc. The friction values were taken at steady state at 10 μm/s from experiments p2280, p2219/p2220, p2222, p2218, and p2284. The critical talc interlayer thickness for the onset of weakening and for "maximum" weakening are indicated. These thresholds are presumably a function of normal stress and the roughness of the talc interlayer surface (e.g., via grain size of the granular quartz in our experiments).

with blue sand which has a slightly larger grain size than our standard granular quartz.

4. Discussion and Implications

[10] Consideration of our complete data set shows that the bulk frictional strength of composite layers decreases systematically with talc interlayer thickness (Figure 3, note that the talc interlayer thickness was corrected for initial compaction). The coefficient of friction ranges from 0.6 to 0.2, which is consistent with existing results for pure quartz and pure talc [*Marone et al.*, 1990; *Mair and Marone*, 1999; *Carpenter et al.*, 2009]. With increasing thickness of the talc interlayer, we find two critical values. The first corresponds to a talc interlayer thickness of ~200 μm and indicates the onset of weakening relative to pure quartz (Figure 3). The second critical thickness is at ~800 μm and corresponds to a fully-weakened layer, with the frictional strength of pure talc. Layers with a talc interlayer thickness between 200 μm and 800 μm exhibit a range of frictional strengths between that for pure quartz and pure talc.

[11] One expects that weakening may vary with layer normal stress, for example due to flow folding of the talc interlayer under shear and enhanced compaction (thinning) of the talc interlayer, and our data show some tendency for this. Increasing the grain size of the sand surrounding the talc fabric resulted in a higher friction for the bulk layer. This is consistent with flow folding of the talc interlayer and deeper penetration, into the talc layer, by larger quartz grains (see auxiliary material). The effect of grain size diminishes with increasing net strain and normal stress, which is consistent with thinning of the talc interlayer, additional grain

penetration, and fabric disruption. Additional work is necessary to understand how these critical thicknesses vary with grain size, boundary roughness for the composite layer, and other factors.

[12] We investigated the effect of fabric on the rate/state frictional properties of the composite layers. Homogeneous mixtures exhibited very similar behavior to that of pure quartz (see auxiliary material). In contrast, the frictional behavior for layers with talc fabric were very similar to that for pure talc. Homogeneous mixtures exhibited "classical" rate and state behavior, with a peak in friction upon an imposed jump in loading velocity followed by a gradual decay to a new steady state value. Layers with talc fabric, however, simply jumped to a new steady state level without any evolution in friction (see auxiliary material for details). All layers exhibited velocity strengthening frictional behavior, but the values of the friction rate parameter, a-b, and the variation with velocity vary with gouge fabric. Homogeneous mixtures exhibited a-b values very similar to those of pure quartz, whereas layers with talc fabric exhibited values similar to pure talc (see auxiliary material for details).

[13] In summary, our mechanical data and observations suggest that the frictional strength of tectonic faults can be extremely low if talc is present in an interconnected network. The degree of weakening depends on the thickness of the weak layer. In nature, talc and most other weak minerals (clays and phyllosilicates) are formed by chemical and hydration reactions [*Imber et al.*, 1997; *Jefferies et al.*, 2006; *Schleicher et al.*, 2006; *Collettini et al.*, 2009b]. Therefore, mature fault zones without inherited weak minerals, should be frictionally strong unless fluids or local chemical reactions produce the weak phases *in-situ*. The formation of such authogenic phyllosilicates and clays has been documented in several settings [*Wintsch et al.*, 1995; *Imber et al.*, 1997; *Holdsworth*, 2004; *Schleicher et al.*, 2006; *Collettini et al.*, 2009b] and grain size reduction and associated reaction rate enhancement is a possible agent to localize the reaction products (e.g., talc) as coatings on the surfaces of strong minerals, ultimately forming a weak through-going foliation.

[14] These observations have important implications for methods of evaluating fault strength and for the strength and evolution of mature, long-lived faults. The importance of accounting for the role of fabric in measurements of frictional strength is clear. Moreover, observations of weak minerals in fault zones coupled with our conclusion that even trace quantities of weak phyllosilicates can induce fault weakness if the minerals form a connected, through-going arrangement indicates that we must understand coupling between fault processes and fabric development [*Evans and Chester*, 1995; *Wintsch et al.*, 1995; *Imber et al.*, 1997]. This is consistent with other observations that zones of active fault slip may be only microns to millimeters in thickness on fault mélanges that are maybe decimeters to 10s of meters wide and have accommodated kilometers of slip during their lifetime [e.g., *Chester and Chester*, 1998; *Schulz and Evans*, 1998]. However, the findings of the present work suggest that mechanical deformation coupled with chemical transformations are necessary ingredients to develop the requisite network of weak minerals that may provide reduced strength at only trace concentrations of the weakening phase. These ingredients are key if such networks are to form, reorganize

and endure during the large-scale offset of faults sustained over long periods.

References

Ampuero, J.-P., and Y. Ben-Zion (2008), Cracks, pulses and macroscopic asymmetry of dynamic rupture on a bimaterial interface with velocity-weakening friction, *Geophys. J. Int.*, *173*, 674–692, doi:10.1111/j.1365-246X.2008.03736.x.

Bos, B., and C. J. Spiers (2002), Frictional-viscous flow of phyllosilicate-bearing fault rock: Microphysical model and implications for crustal strength profiles, *J. Geophys. Res.*, *107*(B2), 2028, doi:10.1029/2001JB000301.

Carpenter, B. M., C. Marone, and D. M. Saffer (2009), Frictional behavior of materials in the 3D SAFOD volume, *Geophys. Res. Lett.*, *36*, L05302, doi:10.1029/2008GL036660.

Chester, F. M., and J. S. Chester (1998), Ultracataclasite structure and friction processes of the Punchbowl fault, San Andreas system, California, *Tectonophysics*, *295*, 199–221, doi:10.1016/S0040-1951(98)00121-8.

Collettini, C., and R. E. Holdsworth (2004), Fault zone weakening and character of slip along low-angle normal faults: Insights from the Zuccale Fault, Isle of Elba, Italy, *J. Geol. Soc.*, *161*, 1039–1051, doi:10.1144/0016-764903-179.

Collettini, C., and R. H. Sibson (2001), Normal faults normal friction?, *Geology*, *29*, 927–930, doi:10.1130/0091-7613(2001)029<0927:NFNF>2.0.CO;2.

Collettini, C., A. Niemeijer, C. Viti, and C. Marone (2009a), Fault zone fabric and fault weakness, *Nature*, *462*, 907–910, doi:10.1038/nature08585.

Collettini, C., C. Viti, S. A. F. Smith, and R. E. Holdsworth (2009b), The development of interconnected talc networks and weakening of continental low-angle normal faults, *Geology*, *37*, 567–570, doi:10.1130/G25645A.1.

Dieterich, J. H. (1978), Time-dependent friction and the mechanics of stick-slip, *Pure Appl. Geophys.*, *116*, 790–806, doi:10.1007/BF00876539.

Di Toro, G., et al. (2006), Natural and experimental evidence of melt lubrication of faults during earthquakes, *Science*, *311*, 647–649, doi:10.1126/science.1121012.

Engelder, T., J. M. Logan, and J. Handin (1975), The sliding characteristics of sandstone on quartz fault-gouge, *Pure Appl. Geophys.*, *113*, 69–86, doi:10.1007/BF01592900.

Evans, J. P., and F. M. Chester (1995), Fluid-rock interaction in faults of the San Andreas system: Inferences from San Gabriel fault rock geochemistry and microstructures, *J. Geophys. Res.*, *100*, 13,007–13,020, doi:10.1029/94JB02625.

Faulkner, D. R., and E. H. Rutter (2001), Can the maintenance of overpressured fluids in large strike-slip fault zones explain their apparent weakness?, *Geology*, *29*, 503–506, doi:10.1130/0091-7613(2001)029<0503:CTMOOF>2.0.CO;2.

Holdsworth, R. E. (2004), Weak faults—Rotten cores, *Science*, *303*, 181–182, doi:10.1126/science.1092491.

Imber, J., R. E. Holdsworth, C. A. Butler, and G. Lloyd (1997), Fault-zone weakening processes along the reactivated Outer Hebrides Fault Zone, Scotland, *J. Geol. Soc.*, *154*, 105–109, doi:10.1144/gsjgs.154.1.0105.

Imber, J., R. E. Holdsworth, C. A. Butler, and R. A. Strachan (2001), A reappraisal of the Sibson-Scholz fault zone model: The nature of the frictional to viscous ("brittle-ductile") transition along a long-lived, crustal-scale fault, Outer Hebrides, Scotland, *Tectonics*, *20*, 601–624, doi:10.1029/2000TC001250.

Jefferies, S. P., et al. (2006), The nature and importance of phyllonite development in crustal-scale fault cores: an example from the Median Tectonic Line, Japan,, *J. Struct. Geol.*, *28*, 220–235, doi:10.1016/j.jsg.2005.10.008.

Lachenbruch, A. H., and J. H. Sass (1980), Heat flow and energetics of the San Andreas fault zone, *J. Geophys. Res.*, *85*, 6185–6222, doi:10.1029/JB085iB11p06185.

Lachenbruch, A. H., and J. H. Sass (1992), Heat flow from Cajon Pass, fault strength, and tectonic implications, *J. Geophys. Res.*, *97*, 4995–5015, doi:10.1029/91JB01506.

Mair, K., and C. Marone (1999), Friction of simulated fault gouge for a wide range of velocities and normal stresses, *J. Geophys. Res.*, *104*, 28,899–28,914, doi:10.1029/1999JB900279.

Marone, C., B. Raleigh, and C. H. Scholz (1990), Frictional behavior and constitutive modeling of simulated fault gouge, *J. Geophys. Res.*, *95*, 7007–7025, doi:10.1029/JB095iB05p07007.

Melosh, H. J. (1996), Dynamical weakening of faults by acoustic fluidization, *Nature*, *379*, 601–606, doi:10.1038/379601a0.

Moore, D. E., and D. A. Lockner (2008), Talc friction in the temperature range 25°–400°: Relevance for fault-zone weakening, *Tectonophysics*, *449*, 120–132, doi:10.1016/j.tecto.2007.11.039.

Moore, D. E., and M. J. Rymer (2007), Talc-bearing serpentinite and the creeping section of the San Andreas fault, *Nature*, *448*, 795–797, doi:10.1038/nature06064.

Niemeijer, A. R., and C. J. Spiers (2005), Influence of phyllosilicates on fault strength in the brittle-ductile transition: Insights from rock analogue experiments, in *High-Strain Zones: Structure and Physical Properties*, edited by D. Bruhn and L. Burlini, pp. 303–327, Geol. Soc. of London, Nice, U. K.

Niemeijer, A. R., and C. J. Spiers (2006), Velocity dependence of strength and healing behaviour in simulated phyllosilicate-bearing fault gouge, *Tectonophysics*, *427*, 231–253, doi:10.1016/j.tecto.2006.03.048.

Niemeijer, A. R., and C. J. Spiers (2007), A microphysical model for strong velocity weakening in phyllosilicate-bearing fault gouges, *J. Geophys. Res.*, *112*, B10405, doi:10.1029/2007JB005008.

Niemeijer, A., C. Marone, and D. Elsworth (2008), Healing of simulated fault gouges aided by pressure solution: Results from rock analogue experiments, *J. Geophys. Res.*, *113*, B04204, doi:10.1029/2007JB005376.

Rice, J. R. (1992), Fault stress states, pore pressure distributions, and the weakness of the San Andreas fault, in *Earthquake Mechanics and Transport Properties of Rocks*, edited by B. Evans and T.- F. Wong, pp. 475–503, Academic, London.

Rutter, E. H., and D. H. Mainprice (1979), On the possibility of slow fault slip controlled by a diffusive mass transfer process, *Gerlands Beitr. Geophys.*, *88*, 154–162.

Schleicher, A. M., B. A. Van der Pluijm, J. G. Solum, and L. N. Warr (2006), Origin and significance of clay-coated fractures in mudrock fragments of the SAFOD borehole (Parkfield, California), *Geophys. Res. Lett.*, *33*, L16313, doi:10.1029/2006GL026505.

Scholz, C. H. (2000), Evidence for a strong San Andreas fault, *Geology*, *28*, 163–166, doi:10.1130/0091-7613(2000)28<163:EFASSA>2.0.CO;2.

Schulz, S. E., and J. P. Evans (1998), Spatial variability in microscopic deformation and composition of the Punchbowl fault, southern California: Implications for mechanisms, fluid-rock interaction, and fault morphology, *Tectonophysics*, *295*, 223–244, doi:10.1016/S0040-1951(98)00122-X.

Scott, D. R., C. J. Marone, and C. G. Sammis (1994), The apparent friction of granular fault gouge in sheared layers, *J. Geophys. Res.*, *99*, 7231–7246, doi:10.1029/93JB03361.

Shea, W. T., Jr., and A. K. Kronenberg (1993), Strength and anisotropy of foliated rocks with varied mica contents, *J. Struct. Geol.*, *15*, 1097–1121, doi:10.1016/0191-8141(93)90158-7.

Wintsch, R. P., R. Christoffersen, and A. K. Kronenberg (1995), Fluid-rock reaction weakening of fault zones, *J. Geophys. Res.*, *100*, 13,021–13,032, doi:10.1029/94JB02622.

Zoback, M. D. (2000), Strength of the San Andreas, *Nature*, *405*, 31–32, doi:10.1038/35011181.

Zoback, M. D., et al. (1987), New evidence for the state of stress of the San Andreas fault system, *Science*, *238*, 1105–1111, doi:10.1126/science.238.4830.1105.

D. Elsworth, Department of Energy and Mineral Engineering, Pennsylvania State University, 231 Hosler Bldg., University Park, PA 16802, USA.

C. Marone, Department of Geosciences, Pennsylvania State University, 536 Deike Bldg., University Park, PA 16802, USA.

A. Niemeijer, Istituto Nazionale di Geofisica e Vulcanologia,Via di Vigna Murata 605, I-00143 Roma, Italy. (andre.niemeijer@ingv.it)